sustainability

MDPI

Article

Implementation of a 3D Coupled Hydrodynamic–Biogeochemical Model in Kuwait Bay

Maria Amélia V. C. Araújo [1,2,*], Luz García-García [2,3] and John Aldridge [2]

[1] Stantec, 50-60 Station Road, Cambridge CB1 2JH, UK
[2] Centre for Environment, Fisheries & Aquaculture Science (Cefas), Pakefield Road, Lowestoft NR33 0HT, UK; luz.garcia@ieo.csic.es (L.G.-G.); john.aldridge@cefas.co.uk (J.A.)
[3] Centro Oceanográfico de A Coruña (COAC-IEO), CSIC, Paseo Marítimo Alcalde Francisco Vázquez, 10, 15001 A Coruña, Spain
* Correspondence: amelia.araujo@stantec.com

Abstract: Production of farmed fish is increasing worldwide and in areas which have traditionally not had large scale farming, specifically regions of high sea temperature. This research presents a methodology to assess the impacts of these developments on water quality and to manage them in the context of other discharges into the marine environment. Kuwait Bay, in Kuwait, is used as a case study for these types of environments, where the impacts of finfish farms are assessed regarding their location by implementing a 3D coupled hydrodynamic–biogeochemical model. The model was validated against a monthly climatology of field data for hydrodynamics and biogeochemical parameters. Results show that the impact of a farm size with an average historical production is minimal, with a slight increase in nutrient concentrations (0.4%) and in chlorophyll-a and oxygen (less than 1%) compared to the baseline (no farm). When the farm was located outside the bay, at the southern coast, the impact was even smaller. This suggests that the flushing conditions of the location are a prime consideration and can help mitigate the impacts of larger farm sizes.

Keywords: Delft3D-FLOW; Delft3D-ECO; marine management; mitigation; farm location; flushing conditions

Citation: Araújo, M.A.V.C.; García-García, L.; Aldridge, J. Implementation of a 3D Coupled Hydrodynamic–Biogeochemical Model in Kuwait Bay. *Sustainability* **2022**, *14*, 8715. https://doi.org/10.3390/su14148715

Academic Editor: Gioele Capillo

Received: 12 June 2022
Accepted: 11 July 2022
Published: 16 July 2022

1. Introduction

The need to assess the environmental sustainability of marine finfish aquaculture is of increasing importance given the projected increases in production needed to support growing human populations and the avoidance of overexploitation of wild fish stocks [1–3]. To support this projected increase in aquaculture, development may be expected to occur in regions without a history of large-scale aquaculture deployments. In fact, the production of farmed fish is increasing in areas which have traditionally not had large scale farming, specifically regions of high sea temperature. However, intensive aquaculture production brings the risk of impacts on the marine environment. This can occur in a number of ways, but a key impact is through the additional quantities of organic and inorganic nutrients entering the water column and benthic system from farmed fish excretion or unconsumed fish feed. If sufficiently large or focused in a small area, this can lead to undesirable consequences such as phytoplankton blooms, oxygen depletion and increased turbidity [4]. Nevertheless, although aquaculture practices in the marine case have resulted in some environmental degradation in areas such as northern Europe, high production with reduced environmental impacts per unit of production has been achieved through a combination of improved feeds and proper siting of farms [4].

Finfish aquaculture in Kuwait Bay, Kuwait, has historically been relatively modest, with Gilthead seabream (*Sparus aurata*), Sobaity seabream (*Sparidentex hasta*) and European seabass (*Dicentrarchus labrax*), commercially produced until 2008. Production in the period 2000–2007 averaged 127 tonnes/year (all species) based on approximately 73 cages

with a total culture volume of about 116,000 m^3, although with considerable inter-annual variability [5]. Massive fish kill events, associated with low dissolved oxygen levels, have occurred in the bay during the summer over the past 20 years [6]. The aquaculture activities using marine cages were closed in 2008 due to these events and have continued to be closed since then [7]. However, in common with many countries, Kuwait is looking to promote the application of aquaculture with the aim of reducing pressure on wild fish stocks and improving future food security, and applications for new production sites are under consideration [7]. In this research, the potential impact of fish farming in the coastal zone of Kuwait Bay is explored using a coupled physical and biogeochemical model. Both previous fish farming sites and a proposed new site are examined for potential impacts of finfish farm waste on nutrients, phytoplankton, chlorophyll-a and oxygen concentrations. This study considers those impacts and how they can be mitigated by farm location.

2. Description of the Study Area

This study is mostly focused on Kuwait Bay but the computational domain extends to other areas in Kuwait: south to Al Khiran and east to about 25 km eastwards from the Shatt Al-Arab river mouth (see Figure 1). Kuwait Bay is located in the northwest end of the Arabian Gulf. The Bay is a shallow water body (average depth 5 m) with the deepest part located at its mouth (23 m). Tides in the bay are mainly semi-diurnal, with maximum tidal ranges of 4.3 m. The sea surface temperatures range between 13 °C in winter and 35 °C in summer, and the salinity oscillates between 41.5 to 47.5 psu, since evaporation rates exceed the net fresh water input obtained by precipitation and river runoff [6,8]. This salinity is significantly above the world's average salinity (35 psu). Desalination plants at the coast, which discharge super saline effluent, and the decrease in the Shatt Al-Arab river runoff (a study [9] estimated the historical discharge in 1456 m^3/s, whereas recent field surveys provided values for discharges ranging from 40 to 70 m^3/s [10]) are believed to have contributed to the extreme values for salinity, which has experienced an increasing trend in the last years (see, for instance, [11]). Although the Shatt Al-Arab river discharges to the Arabian Gulf, historically it had a high impact in Kuwait Bay. The bay also receives significant inputs of raw sewage and partially treated wastewater, particularly from its southern coast [12].

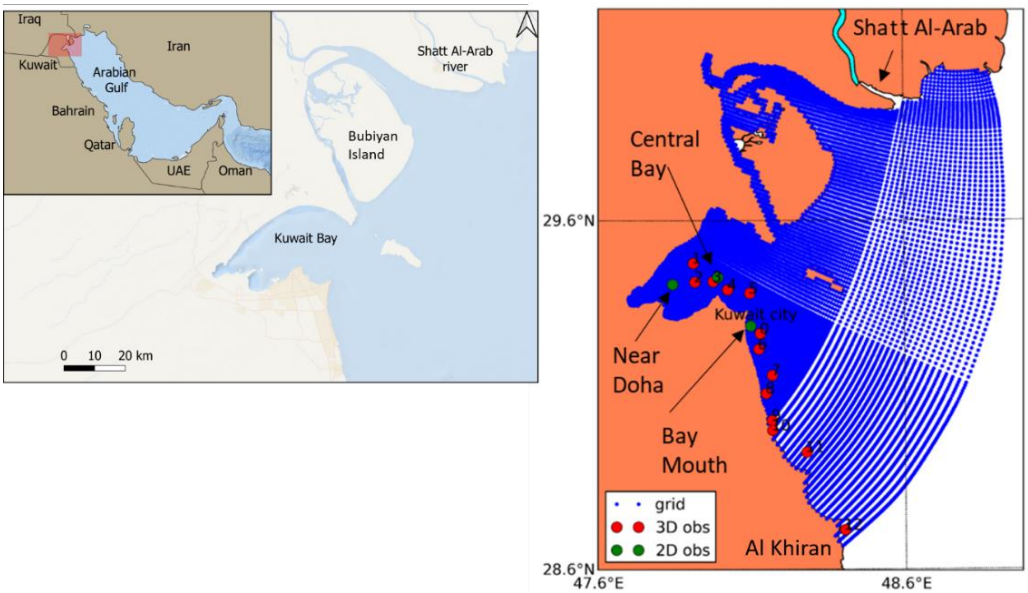

Figure 1. Arabian Gulf, zooming-in of the study area and model domain including Kuwait Bay, where the grid presents a very fine resolution (represented by the blue dots). Observation stations are represented in red (for temperature and salinity) and green (for water levels and/or velocities) dots.

Hydrodynamic studies in the area suggest that the mean water circulation in the bay is governed by the combination of tides, wind and density differences with the upper part of the Arabian Gulf. Observations carried out in the summer of 2012 showed that the Bay was characterized by an overall inverse estuarine circulation [13], which was also reproduced by three-dimensional numerical studies [14]. The hydrodynamic conditions determine the residence time or flushing conditions inside the Bay. This is the time needed for a pollutant discharged at the coast to be transported to offshore locations. Given the environmental pressures at Kuwait Bay, several studies of the flushing capabilities have been carried out using numerical models. For instance, according to one study [8], three flushing regimes can be identified in the bay: (1) fastest flushing in the deeper areas close to the bay mouth, (2) fast flushing at the intertidal areas north of the bay mouth governed by wind-driven currents and (3) relatively slower flushing in the inner part of the bay driven by thermohaline circulation. A more recent study related the reduction in the freshwater discharge of the Shatt Al-Arab river to an increase in the residence times of the inner bay, which would be around 144 days, 60 days more than under high river discharge conditions [10].

From a biological perspective, the phytoplankton biomass and primary production in Kuwait Bay are different going from north to south, with the northern waters showing values around 4.4 mg/m^3 for biomass and 453.4 mgC/m^3 day^{-1} for primary production due to the influence of the Shatt Al-Arab river, compared with the southern waters characterized by values of 1.5 mg/m^3 and 42.2 mg C/m^3 day^{-1}, respectively [15,16]. The phytoplankton biomass in the area is of the same order of magnitude as in other coastal areas in the world, such as the Barrier Island, the southwest coast of India and Venezuela [15].

The factors that limit the primary production in the Kuwait Bay are not well known. There is evidence [17] that the production was not light limited, but nutrients were not likely to be limiting production either since they were rarely depleted. Similar results were reported in another study [15].

The seasonality of the phytoplankton production is not pronounced and does not display the sharp increases in algal biomasses in spring/summer that are characteristic of waters from other regions. However, some slight increase in biomass during the months of March–May, August and October–December has been found [17], which is consistent with the results of other studies [18], although only for stations 0, 7–12 (see Figure 1). Stations 1–6 in the inner bay did not show the same patterns. The absence of a stronger seasonality has been attributed to several potential factors, such as the lack of stratification and turnover associated with seasons, loss due to lateral advection, grazing by zooplankton, including microzooplankton or the bottom fauna, or the degradation via the bacterial loop [15,17].

The seasonality of the phytoplankton community in Kuwait Bay has been characterized by some researchers [18], showing that diatoms were dominant all year, not only in the inner bay, but also in adjacent waters. Dinoflagellate counts increased in February and March, but were generally much less than diatoms.

3. Materials and Methods

3.1. Available Datasets

The stations for which physical and biogeochemical observations were available are shown in Figure 1. The red dots represent the monitoring stations that the Kuwait Environment Public Authority (KEPA) has been sampling for more than 30 years, as part of KEPA's long-term water quality monitoring program (http://www.emisk.org/emisk/ accessed on 5 June 2016). Physical and biogeochemical variables are collected every month (weather permitting) at these sites, including temperature, transparency, pH, salinity, dissolved oxygen, dissolved inorganic nutrients, total suspended solids, chlorophyll-a, nitrate + nitrite (TOxN), ammonia, dissolved inorganic phosphate and silicate. The variability of these environmental parameters at different temporal scales (seasonal to decadal) has been described in some studies [18,19], with the latest focusing on their effect on the variability of phytoplankton communities. For this study, data in the period 1983–2013 were available, and were used for model calibration and validation purposes.

The green dots in Figure 1 depict the locations for which high temporal resolution (5 min) hydrodynamic data were available (tidal velocities and/or water levels). These data, collected by the Kuwait Institute for Scientific Research (KISR), were measured in the period 21 June 2012–16 July 2012, and determined the choice of year 2012 for the model runs. This dataset has been used in the past in different studies for model validation [8,13].

3.2. Hydrodynamic Model Setup

The Delft3D [20] modelling software was used in this work. The model horizontal mesh consisted of a Cartesian grid with 251 × 198 grid points and 9 sigma layers in the vertical. The structured grid was refined at the Kuwait Bay (see Figure 1), with approximately 100 m resolution inshore and 2000 m offshore, and the vertical layers were divided unevenly, with enhanced resolution at the surface and bottom to better capture the nature of the physical processes at these locations. In particular, the thickness of each layer from the surface to the bottom was, respectively, 5, 5, 5, 10, 15, 25, 20, 10, 5% of the total water depth.

The bathymetry data were the same as used in other studies [21], which were based on compilation of a single beam bathymetry survey conducted in May 2014, by the authors, and complemented with digitized sections of a hydrographic chart of the area [22].

The module Delft3D-FLOW was used for the hydrodynamic simulations; the description of the model and governing equations is presented in the Delft3D-FLOW User Manual [20]. The hydrodynamic model ran for the period 2009–2012, with the first three years considered as model spin-up.

The 2009 simulation was initialized with zero velocities and water levels, and a uniform salinity and temperature of 40.27 and 16.5 °C, respectively, obtained as the average for the month of January 2009 of the KEPA's stations described in Section 3.1. The open boundary was divided into 5 segments (seg 1–5 in Figure 2), to allow the imposition of space variable conditions. Tidal forcing was obtained from the OTPS regional product for the Persian Gulf at 1/60 degrees resolution (http://volkov.oce.orst.edu/tides/PerS.html, accessed on 10 July 2016).

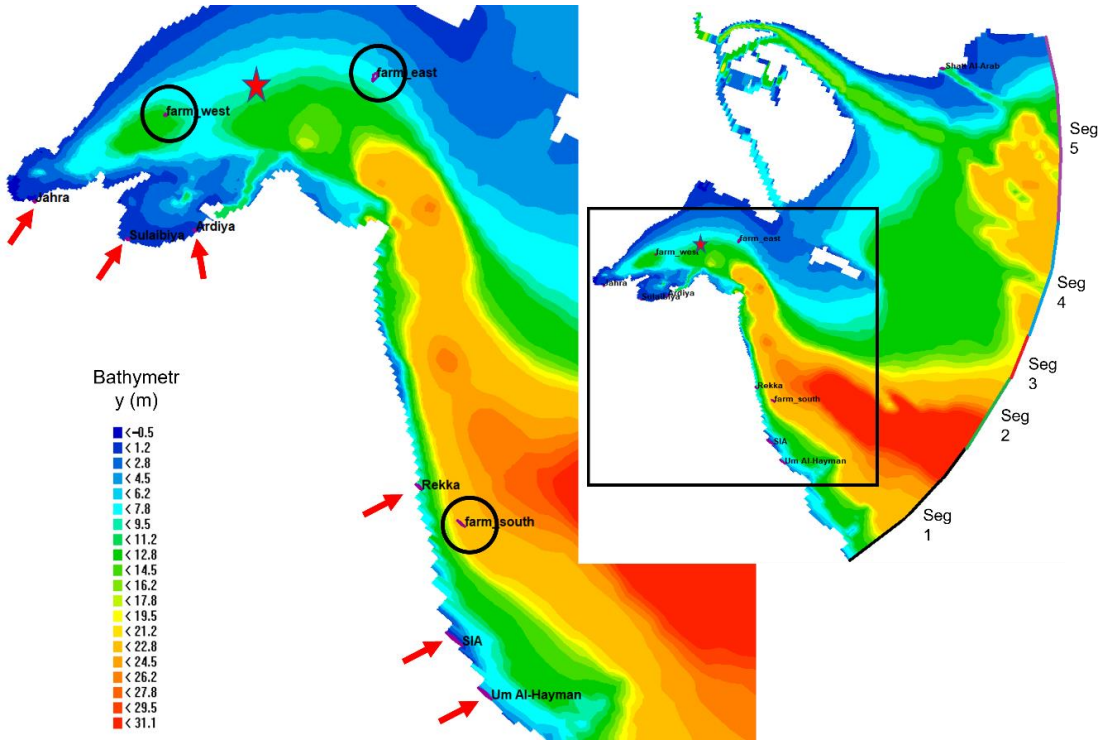

Figure 2. Model domain bathymetry, segmentation of the ocean boundary (5 segments), wastewater discharges (red arrows) and farms location (black circles). The red star represents the location where the meteorological forcing has been extracted.

The forcing for temperature and salinity at the boundary was investigated through a series of preliminary modelling tests (not shown) using either observations measured at station 12 (Figure 1), which is located at the open boundary of the computational domain, and some other approximations, or data from the global ECMWF reanalysis model ORAP5.0 [23] which can be downloaded from http://icdc.cen.uni-hamburg.de/1/projekte/easy-init/easy-init-ocean.html?no_cache=1 (accessed on 15 July 2016). ORAP5.0 has a horizontal resolution of 0.25 degrees and monthly temporal resolution. The idea of using a global model as boundary forcing, despite its coarse resolution, was to account for some spatial variability along the boundary, since observations were only available in the westernmost part of the domain. However, it was soon realized in these sensitivity tests that ORAP5.0 was introducing too much freshwater into the domain, indicating that the Shatt Al-Arab flow rate was based on historical conditions (indeed, based on a research work [24]), not representative of the situation nowadays (see Section 2 for further explanations). Therefore, the selected open boundary conditions were based on observations, with some variability derived from the literature and additional model runs.

The temperature was considered uniform along the boundary and—vertically and was obtained from the monthly climatology for the period 2009–2012 for stations 9–12 (four southernmost stations in Figure 1). The monthly climatology refers to the monthly averages obtained for that period. For salinity, spatially (uniform in depth) and temporally varying (through the year) boundaries were used. The approach for imposing variable salinity along the boundary was as follows: (a) For the southernmost segment (Seg 1 in Figure 2), it was calculated as a monthly climatology between 2009–2012 from stations 9–12 (Figure 1). (b) Since the northernmost segment (Seg 5) is affected by the Shatt Al-Arab plume, its salinity was obtained through a sinusoidal function, following a similar approach from another study [25] for the discharge flow rate, with a maximum value of 38 in October and a minimum of 35 in April, coincident with the minimum and maximum river discharge, respectively. The value of 38 was defined based on the model results from previous research [26], and the value of 35 was obtained from an extra simulation carried out for 2009 considering a free outflow (Neumann boundary condition = 0 or zero gradient) at the open boundary and a river outflow representative of present conditions (see Section 2). This exercise was necessary to estimate the salinities expected to be forced into the domain due to the presence of the river plume, which extends beyond the model boundaries. A computational domain including the whole extension of the Shatt Al-Arab river plume would have been preferable to avoid the estimations above. (c) The salinity values for the remaining segments (Seg 2, 3 and 4) were obtained through a linear interpolation from both the northernmost and the southernmost segments. These boundary conditions were repeated every year for both temperature and salinity.

Meteorological forcing was obtained from the European Centre for Medium-Range Weather Forecasts (ECMWF) ERA-Interim [27]. No spatial variability was considered and hence the winds and all the variables related with the heat flux model (ocean in Delft3D-FLOW), such as relative humidity, air temperature, cloud coverage and net short wave solar radiation, were extracted from a point in the middle of the Kuwait Bay (latitude 29.462 and longitude 47.948), and was assumed to be representative for all the domain.

Based on recent field surveys [10], an annual-mean Shatt Al-Arab river discharge of 60 m^3/s was used (see Section 2). The discharge flow rate was assumed to vary sinusoidally, following the same approach as [25], with a maximum value of 80 m^3/s in April and a minimum of 40 m^3/s in October. The river temperature was considered to vary through the year, according to the values used in another study [28], with a maximum of 32 °C in July and a minimum of 16 °C in December. The average salinity was assumed to be 5 as in other studies [10]. Consistent with the other forcings, the river discharge conditions were applied as a climatology with no interannual variation.

Model Calibration

To improve model performance, some variables were adjusted from the default values, such as the bottom roughness, the viscosity coefficient and a correction factor to the tidal amplitude. Several 2D-runs were carried out combining different values for those variables and the results compared with measured water levels and velocities at different locations (data at the green dots in Figure 1, see Section 2). The model performance was assessed based on the Relative Mean Absolute Error (RMAE) [29], and a rating of "good" ($0.1 < RMAE < 0.3$) was found for the following combination of model parameters: bottom roughness = 0.05 (White-Colebrook formulation), viscosity = 5 m^2/s and an amplitude correction for the tidal constituents of 1.2.

3.3. Biogeochemical Model Setup

The module Delft3D-ECO (BLOOM ECO) was used for the biogeochemical simulations. BLOOM is a multi-species algae model based on an optimization technique that distributes the available resources (nutrients and light) among the algae species [30]. Different groups and/or species of algae can be modelled depending on the particular application, and for each three phenotypes are distinguished by BLOOM: under nitrogen limiting conditions, under phosphate limiting conditions and under light limiting conditions. No grazers (i.e., zooplankton) are considered by default in BLOOM.

A configuration that included the most relevant state variables and processes affecting the biogeochemistry in the area, both in the water column and at the water/sediment interface (i.e., sedimentation and resuspension) was implemented in this study. In particular, the variables (substances) included were: dissolved oxygen (OXY), ammonium (NH4), nitrate (NO3), phosphate (PO4), dissolved silica (Si), opal-Si (opal), particulate organic carbon (POC), particulate organic nitrogen (PON), particulate organic phosphorus (POP), dissolved organic carbon (DOC), dissolved organic nitrogen (DON), dissolved organic phosphorus (DOP), diatoms (considering the three phenotypes of nutrient and light limitation described above), flagellates (the three phenotypes), carbon detritus in the sediment (DetCS1), nitrogen detritus in the sediment (DetNS1), phosphorous detritus in the sediment (DetPS1) and silica detritus in the sediment (DetSiS1). Figure 3 represents the conceptual diagram of the biogeochemical model, including the most relevant active processes.

BLOOM has been validated in a wide range of both fresh water and marine systems [30] and therefore it is believed that the default parametrizations for the algae groups offered by the model could be representative of different environments. However, the default values did not reproduce the observations in Kuwait Bay and a series of modifications to the parameters were necessary to adjust the model results to the observations.

Table 1 shows the parameters used for each of the phytoplankton functional groups and phenotypes with respect to the default ones. The light extinction coefficient was lowered more than 10 times to avoid light limitation in the model (the literature shows that the system is not light limited—see Section 2). Additionally, the default background extinction coefficient (0.08) was changed to 0.04 and the specific extinction coefficient for POC was reduced from 0.1 to 0.001 m^2/gC.

The nitrogen/carbon and silicon/carbon ratios were lowered (proportionally based on the default values) to reduce the uptake of these nutrients from the environment, which are rarely depleted. To further guarantee that a minimum amount of ammonium and phosphate would not be consumed, a threshold concentration for their uptake was prescribed at 0.05 gN/m^3 and 0.015 gP/m^3, respectively. Finally, the mortality of flagellates was increased to keep their biomasses at much lower values than diatoms all along the year, which is in accordance with the observations (see Section 2). It must be remarked that other combinations of parameters would possibly lead to similar results.

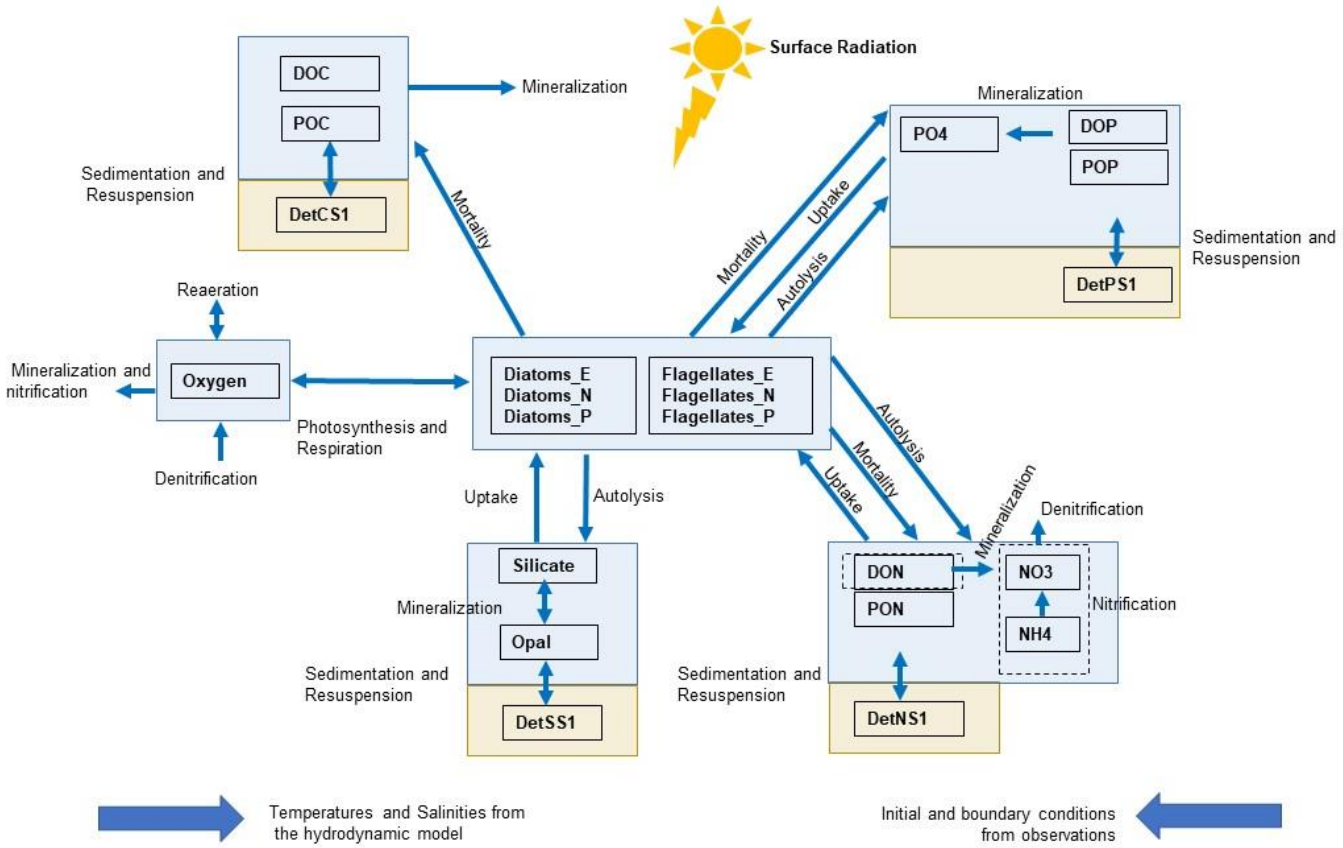

Figure 3. Schematic of the biogeochemical model considered in this study (variables: in boxes; processes: through arrows). The blue rectangles represent variables occur in the water column and the yellow ones refer to the sediment. External inputs to the model are indicated by thick blue arrows and are described at the bottom.

Table 1. Parameters used in the BLOOM simulations versus the default ones for the different phenotypes (E, N, P—under light, nitrogen and phosphorous, respectively, limiting conditions) of diatoms and flagellates.

	Extinction Coefficient (m^2/mg C)	Nitrogen/Carbon Ratio	Silicon/Carbon Ratio	Mortality (day^{-1})
	Default | Used	Default | Used	Default | Used	Default | Used
Diatoms-E	0.24 | 0.0192	0.255 | 0.204	0.447 | 0.00894	0.07 | 0.07
Diatoms-N	0.21 | 0.0168	0.07 | 0.056	0.283 | 0.00566	0.08 | 0.08
Diatoms-P	0.21 | 0.0168	0.105 | 0.084	0.152 | 0.00304	0.08 | 0.08
Flagellates-E	0.25 | 0.02	0.2 | 0.16	0 | 0	0.07 | 0.28
Flagellates-N	0.225 | 0.018	0.078 | 0.0624	0 | 0	0.08 | 0.32
Flagellates-P	0.225 | 0.018	0.113 | 0.0904	0 | 0	0.08 | 0.32

The biogeochemical model was run offline using the same grid as the hydrodynamic model and was forced with the hydrodynamic model results. Simulations were performed for 2012, including 2 years spin up (2010 and 2011), and the daily averaged solar radiation was considered, excluding the night period.

The cold start initial and boundary conditions for the biogeochemical model are compiled in Table 2. These values were based on previous studies [13,31]. In particular, opal, POC, PON, POP, DOC, DON and DOP were fixed at the values used by other researchers [31]. The inorganic nutrients (ammonium, nitrate, phosphate, and silicate) were adjusted through a calibration procedure using the values from previous studies [13]

as a first guess. The initial conditions were set for 2010. The boundary conditions were considered constant along the open boundary and over the 3 years of simulation.

Table 2. Cold start initial and boundary conditions for biogeochemical model.

Nutrient	Concentration (g/m^3)
DO	6
NH4	0.09
NO3	0.0075
PO4	0.02
Si	0.2
Opal-Si	0.1
POC and DON	0.4
PON	0.06
POP	0.006
DOC	5
DOP	0.04

The Shatt Al-Arab river is one of the nutrient sources in the domain. The river nutrient concentrations used in the water quality model are shown in Table 3 and were obtained from different sources: for nitrates + nitrites, phosphates and silicates, averaged values between October 2009 and August 2010 were considered from a study [32]; for ammonium, mean concentrations were used from another study [33]; the remaining nutrients were based on other research work [31], considering 100 times the concentrations of their initial conditions.

Table 3. Flow rate (m^3/s) and nutrient concentration (g/m^3) for Shatt Al-Arab river and the 6 wastewater discharges (see data sources above).

	Shatt Al-Arab River	SIA	Jahra	Rekka	Um Al-Hayman	Sulaibiya	Ardiya
Flow rate	60	0.7	0.25	0.65	0.018	1.61	0.97
DO	6	0	2	2	2	2	2
NO3	0.01691	0.3835	4.198	4.198	4.198	4.198	4.198
PO4	0.00293	18.32	8.1425	8.1425	8.1425	8.1425	8.1425
SiO2	0.04447	0	0	0	0	0	0
NH4	0.002	0.928	0.2695	0.2695	0.2695	0.2695	0.2695
Opal-Si	0.001	0	0	0	0	0	0
POC	40	0	0	0	0	0	0
PON	6	0	0	0	0	0	0
POP	0.6	0	0	0	0	0	0
DOC	500	158.42	49.1775	49.1775	49.1775	49.1775	49.1775
DON	40	13.06	4.87	4.87	4.87	4.87	4.87
DOP	4	0	0	0	0	0	0

Besides the river discharge, 6 main wastewater discharges were considered (see Figure 2), based on a study [34]: 5 from sewage treatment plants located in the Bay (Jahra, Sulaibiya and Ardiya) and along the south coast (Rekka and Um Al-Hayman), and one discharge from the SIA—Shuaiba Industrial Area, which includes refineries, petrochemical companies, power plants, a liquefied petroleum gas plant and many small plants. The discharge and nutrient concentration data considered in the model, assumed to be continuous and constant along the time, are compiled in Table 3 and were obtained as follows.

According to some studies [35], about 31% of treated effluent in Kuwait is discharged into the sea. Thus, for the 5 sewage treatment plants assuming they operate at full capacity, the flow rates discharged into the sea were calculated as 31% of their capacity, which was obtained from a previous study [34], except for Ardiya whose capacity was based on

other sources [36]. For the SIA, the flow rate estimates presented in one study [34] were considered, which include both sanitary and industrial wastewater.

Unfortunately, the concentration of nutrients was not available for each wastewater plant and information was only found for Sulaibiya and Ardiya. For these two plants, the concentration for the raw and the secondary treated wastewater was previously published [12]. Therefore, for the purposes of this modelling study, the concentration of nutrients for untreated and treated waters used for all the wastewater plants was defined as the average of the values in Sulaibiya and Ardiya for these type of effluents, respectively.

It is estimated that around 25% of the sewage from wastewater plants is discharged untreated [35]. Hence, the concentration of nutrients at the 5 sewage treatment plants considered in this study was calculated as "0.75 × concentration of treated waters + 0.25 × concentration of untreated waters", with the concentrations for the treated and untreated waters defined above. For the SIA, it was considered that no treatment at all was applied to the wastewater [34], and its concentration was assigned to that of the untreated waters. Finally, since ammonium, dissolved organic carbon and dissolved organic nitrogen concentrations were not available, some assumptions had to be made: ammonium was calculated from the Kjeldahl nitrogen, ammonia and organic nitrogen; total organic carbon (TOC) was calculated from the chemical oxygen demand (COD) considering a COD/TOC ratio of 2.81 (3:1 mass ratio found in wastewater—see, for instance [37,38]), then the DOC was considered to be the same value as the TOC, assuming that DOC accounts for 96% of TOC according to a study carried out in lakes [39]; all the organic nitrogen was assumed to be dissolved and therefore, the DON was assumed to be the same as the total organic nitrogen (TON).

3.4. Modelling Finfish Farms

The impact of finfish farms in Kuwait Bay was investigated considering the location of the farms. Three similar size farms were modelled, two located inside the bay, where the flushing conditions are expected to be relatively low (see Section 2), and a third one located outside the bay in deeper water and subject to a faster flushing (see Figure 2). The farms within the bay are referred to as farm_west and farm_east, based on their respective locations, and the most southerly farm outside the bay was termed farm_south. The farms size corresponds to the average historical farm production in the period 2000–2007. The farm_west is at an approximate location of the 73 cages referred in Section 1.

The three farms were considered to be of equal size and produce the same nutrient discharge. Because they were located in different water depths with different model grid cell areas (Table 4), the grid cell volume at each location was different. To provide consistency, the assumed number of grid cells occupied by each farm was adjusted so that each farm was discharging the same nutrients in approximately the same volume. Organic particulate waste was assumed to settle rapidly to the bottom, so the organic material was introduced in the model bottom layer, which represented 5% of the water column. Dissolved inorganic nutrient inputs were introduced in the model surface layer where the cages are situated. The percentage occupied by the bottom layer of the model was accounted for when calculating the grid cell volume corresponding to each farm, which is shown in Table 4.

Table 4. Water depth, cell area and cell volume for each farm.

	Water Depth (m)	**Cell Area (m^2)**	**Cell Volume (m^3)**
Farm_west	11.8	7.6621×10^4	45,091
Farm_east	7.3	5.6295×10^5	206,039
Farm_south	22.3	1.8478×10^5	205,660

As shown in Table 4, farms east and south have comparable cell volumes. However, since the farm_west cell volume is much smaller, the corresponding nutrients needed to be

released in a different way, spreading their mass into five adjacent cells, performing a total volume of 204,74 m^3, which is now comparable with the other two farms.

Nutrients associated with fish farm waste enter the environment by three main pathways: (1) as fish feces (mainly organic, particulate); (2) in fish urine (mainly inorganic, dissolved); (3) as unconsumed fish feed (organic, particulate). Input from feed waste (pathway 3), in poorly managed farms, can be 20% to 40% of the total feed input [40,41]. However, modern practice in well-managed farms can drastically reduce loss and, for example, [42] assumed a value of only 3% for salmon farm feed waste in their modelling. In this study a well-managed farm practice was assumed with no fish feed waste. Input was therefore solely via pathways 1 and 2.

Estimates of the nutrient inputs were based on experimental data for Gilthead seabream [43], a fish species previously farmed in the region [5]. Values expressed as nutrient inputs entering the environment per tonne of production were multiplied by the average historical production (127 tonnes y^{-1}) to give an annual load (Table 5). The BLOOM ECO model requires inputs to be specified as a flow rate and associated concentration, so loadings were converted to concentrations assuming a nominal flow rate of 1 m^3/s. Model results were checked and confirmed to be independent of the flow rate as long as total input load was the same. The model also requires organic carbon values for the particulate organic inputs. Salmon feces C:N ratios (by weight) were reported to be in the range 10:1–16:1 [44]. In the simulations here, a C:N ration of 10:1 was used.

Table 5. Carbon and nutrient inputs per farm as used in this study.

	Waste Input (kg per Tonne of Fish Production)	**Annual Input Assuming 127 Tonnes/Year Production (Tonnes y^{-1})**
PON	21	2.67
DIN [1] (as ammonium)	73	9.27
DON	1	0.13
POP	9	1.14
DIP [2] (as phosphate)	7	0.89
DOP	0	0.00
POC	210	26.67
DOC	7	0.89

[1] Dissolved inorganic nitrogen; [2] Dissolved inorganic phosphorous.

4. Results

4.1. Hydrodynamic Model Validation

Figure 4 shows the model results against measured water levels (Near Doha) and tidal velocities (Central Bay and Bay Mouth) for the three stations marked in green in Figure 1, for the period 24 June 2012–28 June 2012. Each plot shows the RMAE, which was "good" in all the cases.

The model validation for temperature and salinity at the surface was performed by comparing the simulation results with a monthly climatology of the observations at station stZ03 (Central Bay) in the period 1983–2013 (Figure 5). The standard deviation around the mean is shown for all the months in order to account for the range of variability in the observations. Qualitatively, the model was able to reasonably reproduce the average seasonal variability of temperature and salinity. The range of variability for temperature was small, compared to that for salinity, and for most of the year the model results fell within this range, except for the spring months, when a slight overestimation was observed. The modelled salinity remained within the limits of variability of the observations throughout the year.

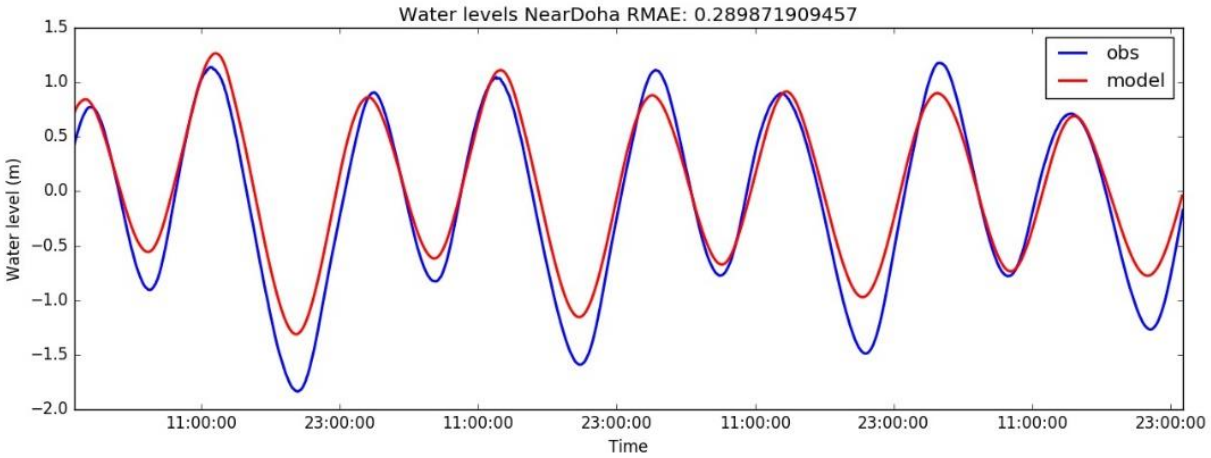

(**a**)

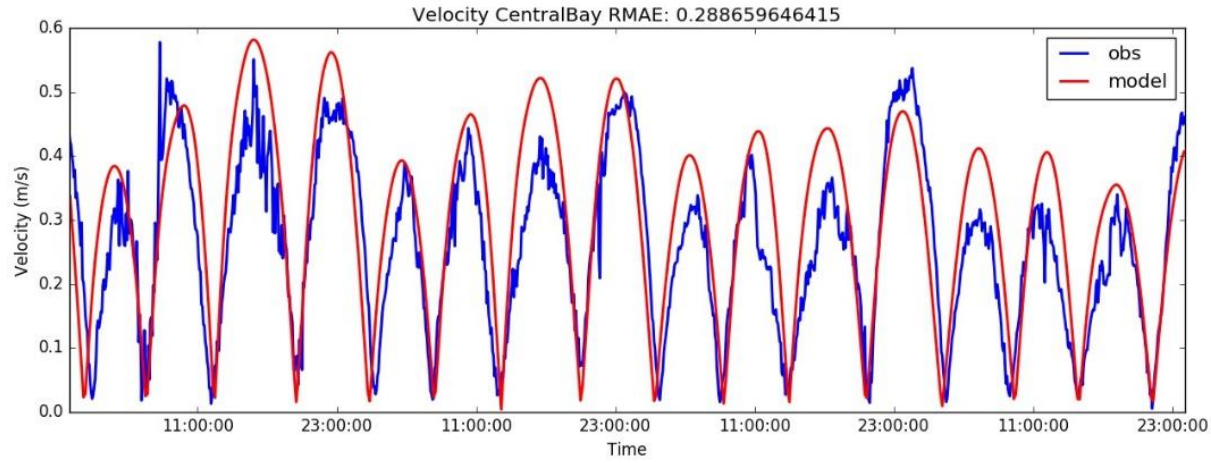

(**b**)

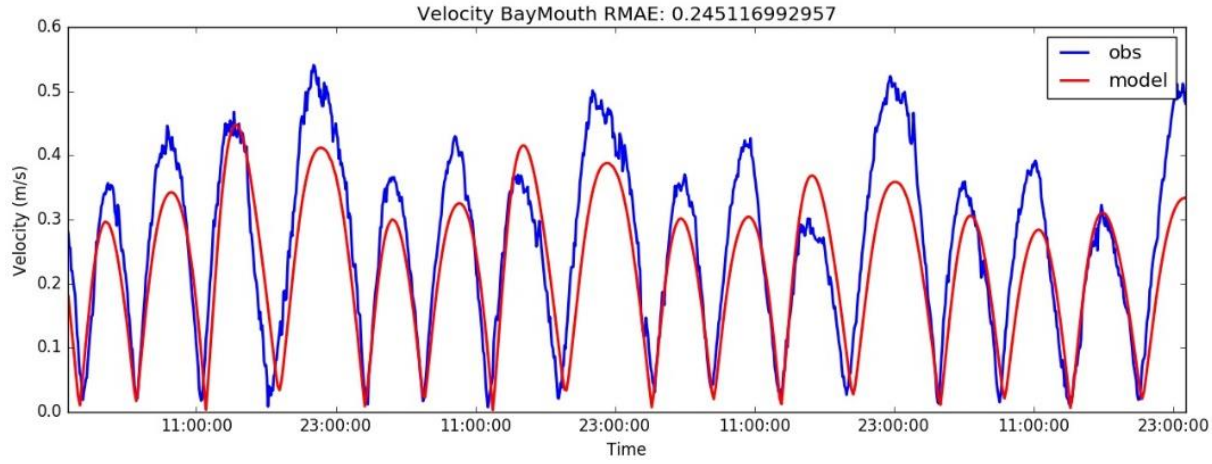

(**c**)

Figure 4. (**a**) Observed and simulated water levels at the station Near Doha; (**b**) observed and simulated velocities at Central Bay; (**c**) observed and simulated velocities at Bay Mouth.

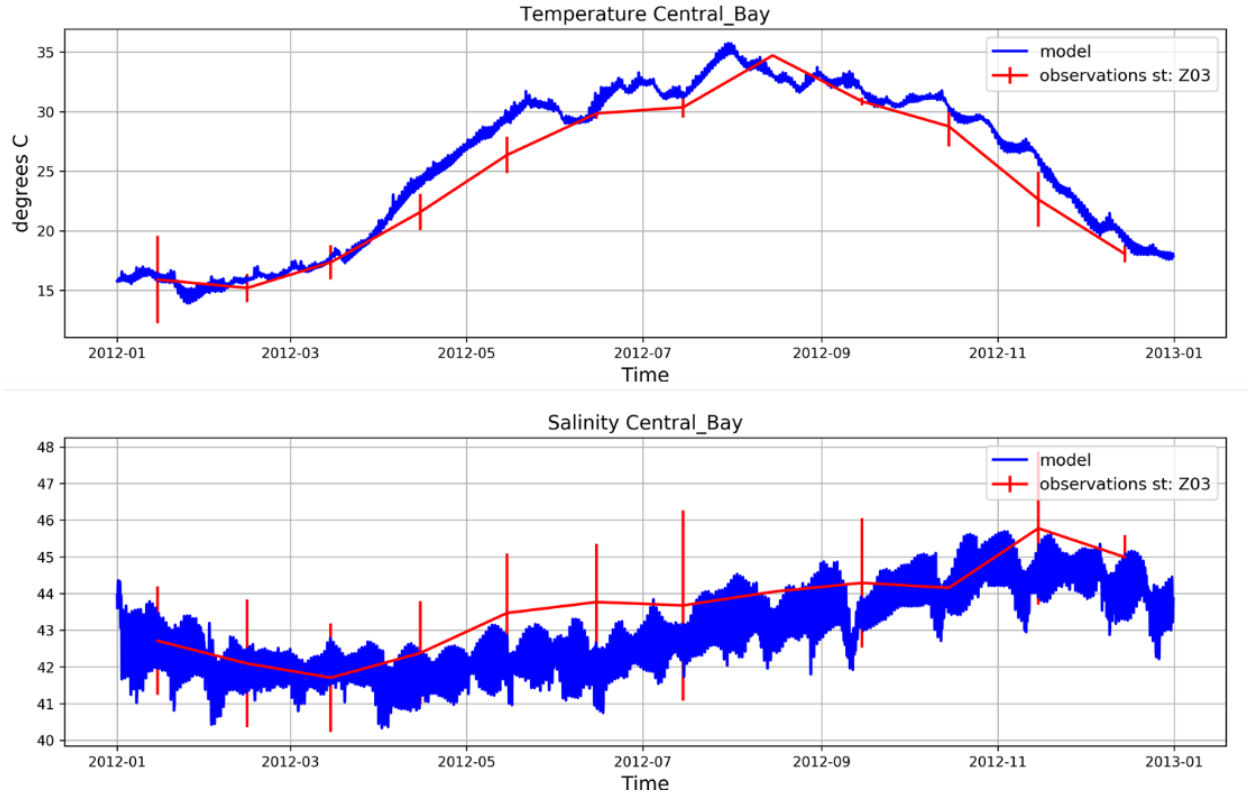

Figure 5. Observed and simulated sea surface temperatures (**top** panel) and salinities (**bottom** panel) at station Central Bay.

4.2. Biogeochemical Model Validation

Figure 6 shows the comparison of the model results at the Central Bay station (stZ03) with the observed average monthly values for chlorophyll-a, dissolved oxygen and nutrients (nitrate, ammonium, phosphate and silicate). Interannual variability is indicated by the superimposed 95% confidence intervals (outliers below the 2nd percentile and above the 98th percentile were removed to produce these plots). Due to the so-called Mishref event, where a malfunction at the Mishref pumping station caused raw sewage to be discharged into the sea from August 2009 to July 2012 [19], averaged observations for the whole time period (1983–2013) and the period previous to the Mishref malfunctioning event (1983–2008) are shown. The data available for the simulated year (2012) were also plotted by means of black stars. Regarding the observations, it is interesting that the 1983–2013 and 1983–2008 climatologies are very similar for all the variables apart from ammonium, for which the 1983–2013 climatology shows much higher values, probably reflecting the consequences of the Mishref event.

Focusing on the comparison between model and observations, we can see that for chlorophyll-a (Figure 6a) the model overestimates the climatologies, especially during the summer (coinciding with the highest temperatures). For the rest of the year, the values remain within the observed variability, and generally below 3 mg/m^3. The observations for 2012 are in the lower end of the measured values (around 1 mg/m^3 through the year). Oxygen concentrations showed a pronounced seasonal variability driven by the temperature differences, with higher values in winter and lower values in summer (Figure 6b). Since the model well-represented the seasonal signal of temperatures (Figure 5, top panel), it also reproduced the monthly variability of oxygen well.

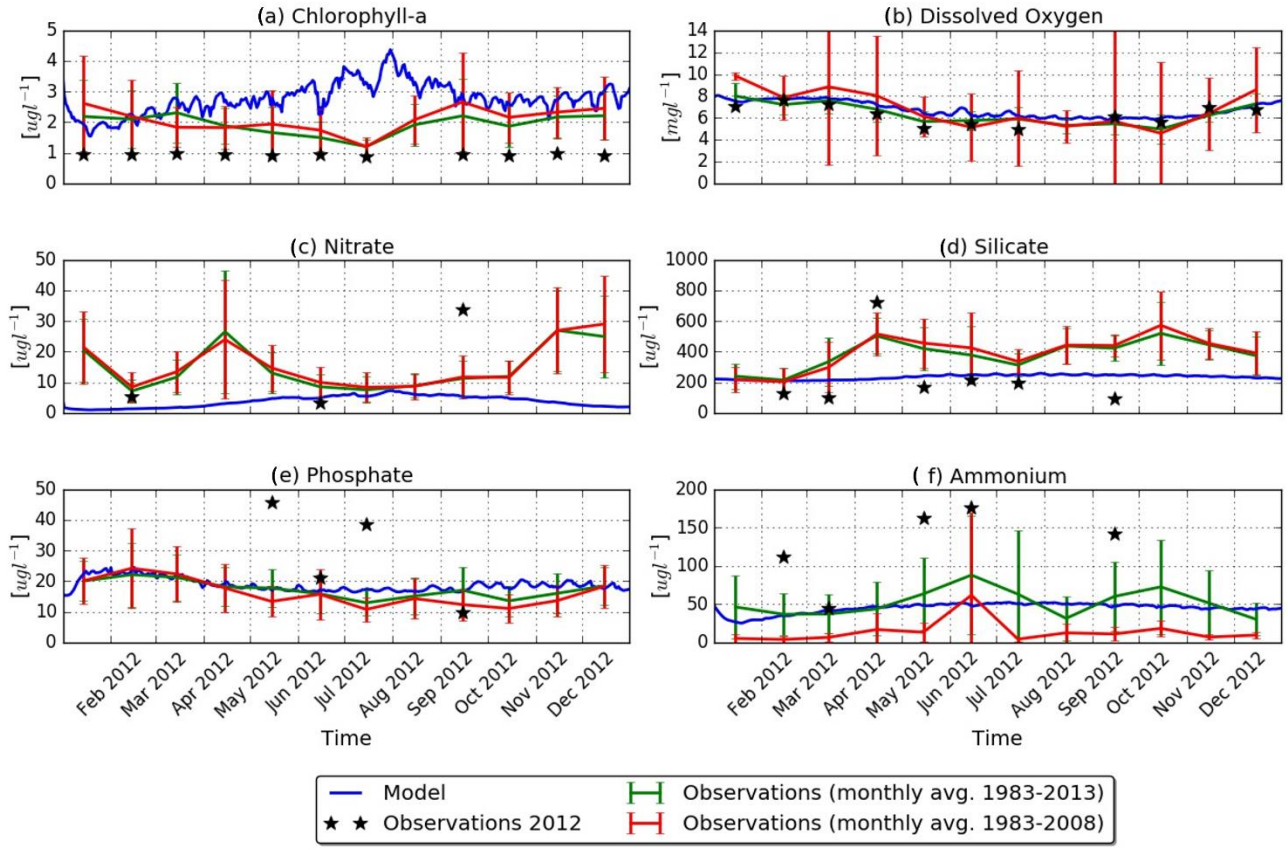

Figure 6. Observed and simulated chlorophyll-a, nitrate, phosphate, dissolved oxygen, ammonium and silicate at station Central Bay, stZ03 (see Figure 1). Model results are referred to 2012. The monthly averaged observations for 1983–2013 and 1983–2008 correspond to the whole period and the period before the Mishref event, respectively.

The observed concentration of nitrate showed a certain seasonality, with higher values in spring and winter, but with a wide range of variability (Figure 6c). The model was not able to reproduce this seasonality, and consistently underestimated the averaged observations, although it remained within the range of variability between June and October. Low values, similar to those obtained by the model (<10 mg/m^3), were measured in the months of February and June 2012, although a strong peak was registered in September, which was not captured by the model.

The model underestimated the concentration of silicate for most of the simulation period (except for the months of January and February), being around 200 mg/m^3, while the averaged observations reached values of 400 mg/m^3 and higher, although with significant variability (Figure 6d). The observations for 2012 remained generally at the level of the model results or lower, apart from in April, which showed a peak of around 700 mg/m^3. Modelled phosphate was close to the observed averaged concentrations, although for year 2012 high values were measured in May (approximately 45 mg/m^3) and July (40 mg/m^3) that were not captured by the model (Figure 6e). The modelled concentration of ammonium remained almost constant throughout the year at around 50 mg/m^3 matching the concentrations averaged over the period 1983–2013. However, except for the month of March, the observations for 2012 registered values between two and three times higher, probably associated to the Mishref event.

The spatial distribution of the annual averaged chlorophyll-a and dissolved oxygen at the surface for 2012 is depicted in Figure 7. Focusing on Kuwait Bay, highest chlorophyll-a concentrations (>10 mg/m^3) occur in coastal areas, especially in the neighborhood of the wastewater discharges, where nutrient inputs are higher (see Figure 2). The concentration in

the bay interior and mouth is between 1 and 3 mg/m^3, in agreement with the observations reported in other work [45]. Nutrient inputs through the Shatt Al-Arab river and, to a minor extent, through the wastewater plants in the southwestern coast are clearly reflected by higher chlorophyll-a concentrations around these sources.

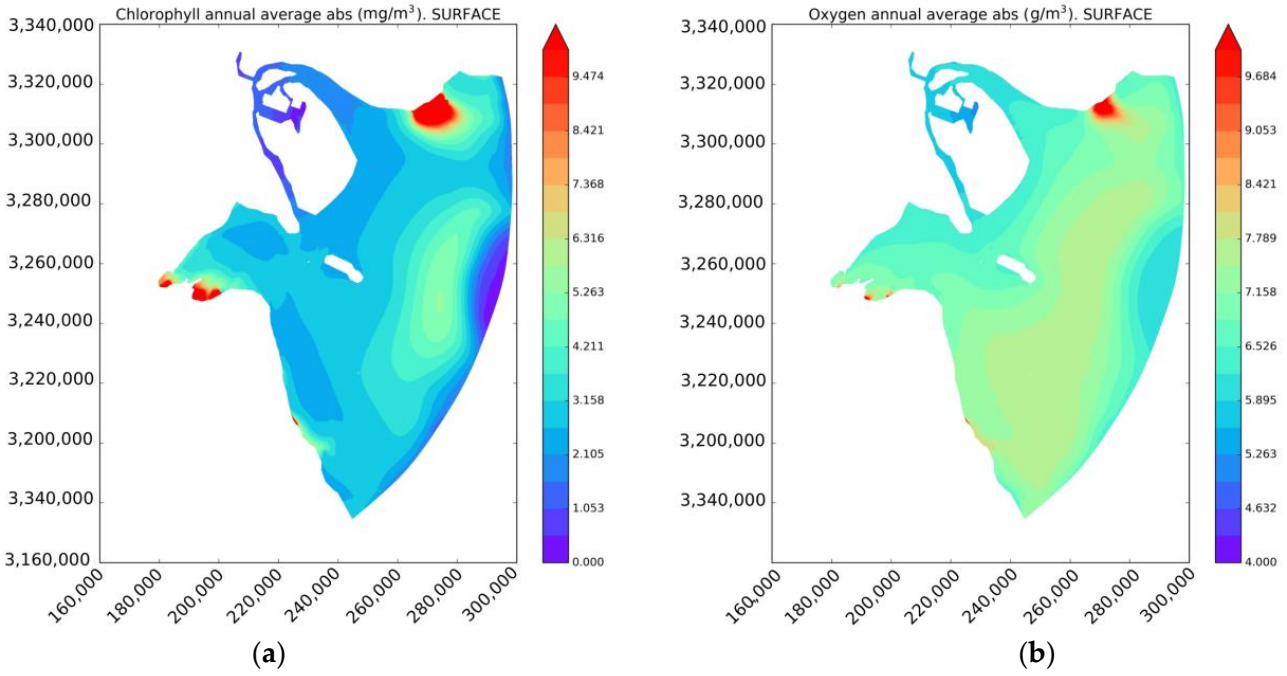

Figure 7. Surface results for 2012: (**a**) annual averaged concentration of chlorophyll; (**b**) annual averaged dissolved oxygen.

The concentration of dissolved oxygen is also higher where nutrient inputs are higher (see Figure 7b), in agreement with the observations from other studies [45] for Kuwait Bay. Concentrations of around 7 g/m^3 are predicted in the inner bay and at its mouth, which is within the range of observed values [45].

4.3. The Effect of Finfish Farms

The percentage change between the baseline simulation (no finfish farms) and the simulation based on the historical farm size is shown for annual average ammonium, nitrate, chlorophyll-a and oxygen at the seabed (Figure 8).

The predicted effect on the average nutrient concentrations was minimal. Ammonium at the seabed close to the farms increased by less than 0.4%, with largest effects near farm_west inside the Bay, due to the low flushing characteristics in this area (see Section 2). Increases at farm_east, and especially at farm_south, were lower, probably due to being situated in a better flushed area (see Figure 8a). As referred to before, farm_south was placed outside the Bay, in deeper water, subject to a faster flushing. Maximum nitrate increases of 0.4% occurred at the northern coast and at the channel situated to left of Bubiyan Island (Figure 8b). This increase in the concentration of nutrients slightly raised the concentration of chlorophyll-a (less than 1%), this increase being more intense inside the bay in accordance with the flushing characteristics mentioned above (Figure 8c). Oxygen concentration was also slightly higher (less than 1%) at farm_west due to the increase in phytoplankton production. Changes in oxygen concentration at the other two farms were almost negligible (Figure 8d).

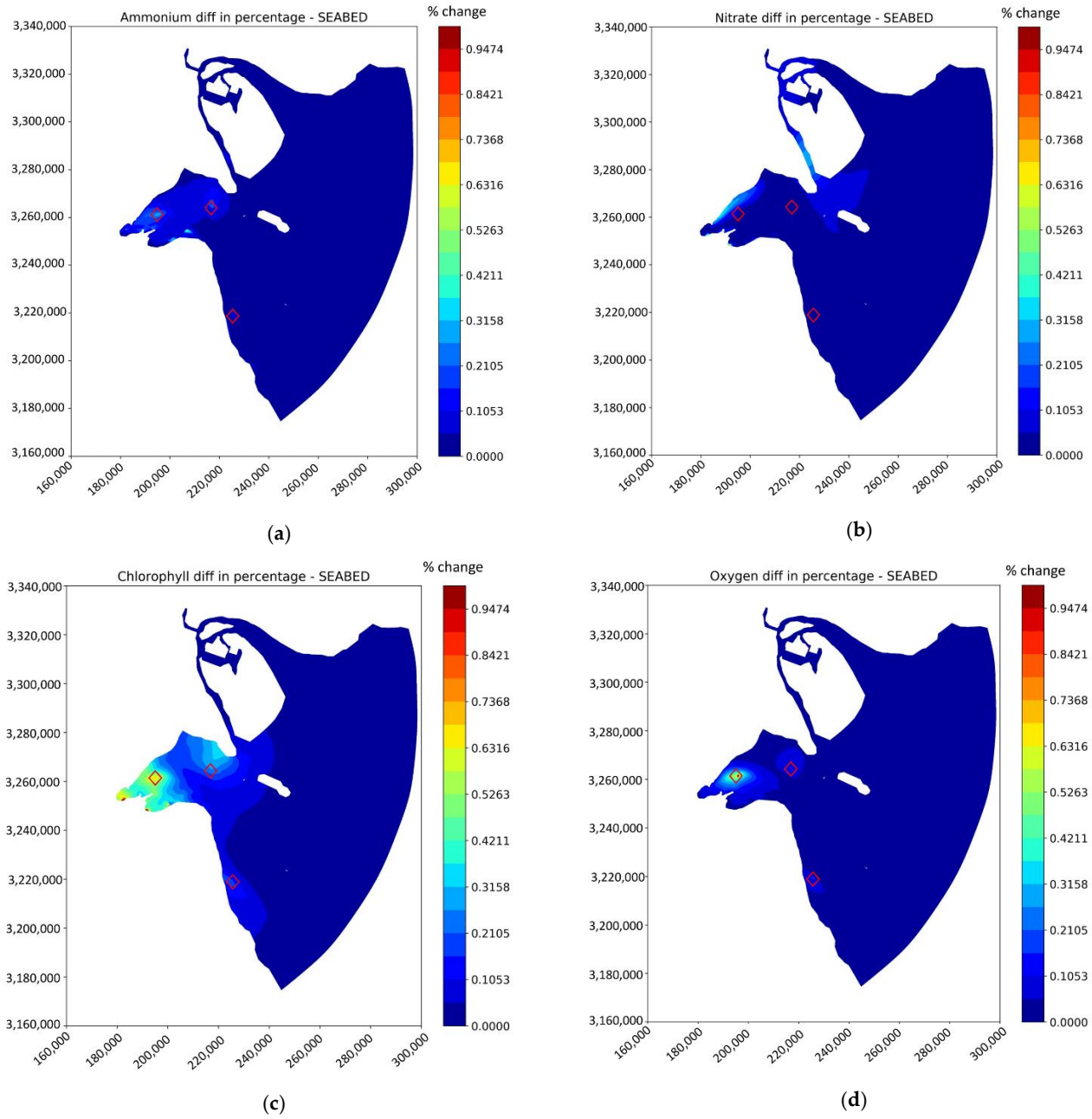

Figure 8. Percentage change compared to the baseline (no farms): (**a**) ammonium; (**b**) nitrate; (**c**) chlorophyll-a; (**d**) oxygen. The 3 modelled farms locations are represented by red diamonds.

5. Discussion

5.1. Biogeochemical Model Results

The biogeochemical model presented here was able to broadly reproduce the observed averaged annual cycle of concentrations for chlorophyll-a, phosphate and ammonium (when averaged over the period 1983–2013), but underestimated the values of nitrate and silicate. However, for these two nutrients, the obtained concentrations were reasonable within the variability of the observations and the measurements available for year 2012. The variability of dissolved oxygen was reproduced well at monthly scales.

Modelling the biogeochemistry of the Kuwait Bay is challenging. Of the most important sources of nutrients into the system: the inputs from the Shatt Al-Arab river, and the sewage outfalls discharging directly into the marine environment, we only partially accounted for the Shatt Al-Arab discharges and could give only a rough approximation of

the treated sewage outfalls because of limited information on treatment and the occurrence of illegal discharges with no treatment at all (see [18] and references therein). Moreover, given the scarcity of data, several assumptions on the variability of the inputs into the system were necessary, i.e., monthly sinusoidal discharge for the Shatt Al-Arab, or constant discharges for the published sewage outfalls, as well as on the concentration of nutrients. Thus, any peaks on the observations would not be reproduced, since no particular changes at short time scales were forced into the model. In addition, Kuwait Bay environmental conditions are extreme, with very high temperatures and salinities. It is likely that some of the parameters used in the model were obtained in milder conditions, and might not be appropriate for the ranges observed in the bay.

The model results presented here were produced considering the most appropriate forcings for the period modelled, e.g., a reduced Shatt Al-Arab river discharge. In this sense, the comparison with the climatologies shown in Figure 6 is not fully homogeneous, since the climatologies reflect an average over a period of 30 years in which the Shatt Al-Arab flow rate has dramatically decreased (see, for instance, the historic review of flow rates in [10] or [19]), almost certainly producing significant changes in nutrient inputs. Furthermore, the malfunctioning of the Mishref pumping station released substantial amounts of untreated sewage into Kuwait Bay from 2009 up to 2012. None of these medium/long-term processes are included in the model presented here.

Nevertheless, the results appear comparable or better than those in previously reported biogeochemical/water quality modelling studies in the region. For example, results of a Delft3D-WAQ model for Kuwait Bay [13], compared with observations at short time scales (27 June—10 July 2012), roughly reproduced the spatial variability but not the peaks of nutrients, possibly induced by dust storms and not accounted for in the model. Another study [31] showed the validation of a 3D Delft3D-WAQ (BLOOM module) for the Arabian Gulf against observations offshore of Kuwait. Only the variability of dissolved oxygen was reasonably reproduced. A Delft3D-WAQ model (DYNAMO module) has recently been implemented to investigate the processes governing the formation of hypoxic water parcels in Kuwait Bay [6]. A detailed and successful validation for oxygen was provided, however other biogeochemical variables were not shown, preventing a comparison with the results of our study.

5.2. Finfish Farms Results

The results presented here suggest that the relatively small-scale finfish production historically sited inside Kuwait Bay would only cause minimal increases in nutrient concentrations and biological production. Given that the concentration of oxygen at the bottom slightly increased with respect to the baseline scenario, hypoxia events caused by the degradation of an excess of accumulated organic matter are not expected to occur. Additionally, since this is a shallow region with no light limitation, the phytoplankton might be able to grow near the seabed. Notice that these results were obtained considering the mineralization rates provided by default in DELWAQ, since no other information was found for the study area in the literature. Faster mineralization rates would impact the results by decreasing the concentration of organic matter at the seabed and subsequently, the concentration of oxygen, but further research is needed to properly quantify this process. Although based on a different modelling approach, the importance of the parametrization of the processes taking place at the seabed (in particular, the sediment oxygen demand) required to reproduce the observed concentration of oxygen has been highlighted [6].

Another important outcome of this study is that the environmental impact of the finfish farms significantly decreases when they are installed in areas with shorter water residence times (such as the southern coast of Kuwait). In this way, the impacts of larger farm sizes can be mitigated by choosing a better flushed location. This would support, for instance, the suitability in environmental terms of the Al Khiran area as a potential site for farming. The official declaration of this site for aquaculture is under way [7].

6. Conclusions

A three-dimensional offline coupled hydrodynamic–biogeochemical model system was implemented for Kuwait Bay using Delft3D-FLOW and Delft3D-ECO models. The model was validated against a monthly climatology of field measurement data, corresponding to physical and biogeochemical observations for more than 30 years. The hydrodynamic simulations ran for the period 2009–2012, with the first three years considered as model spin-up. The biogeochemical model used BLOOM, a multi-species algal model, where the most relevant state variables and active processes were included, and the simulations were performed for 2012 including the two previous years as a spin-up. The model was able to reproduce the hydrodynamics of the bay well and to roughly reproduce the values for chlorophyll-a, phosphate and ammonium. Despite the concentrations of nitrate and silicate being underestimated compared to the monthly averaged observations, they were within the observed variability and the measurements available for 2012.

The validated model was used to investigate the impact of finfish farms in Kuwait Bay, taking into account their location. Three similar size farms were modelled: two located inside the Bay (in poor or relatively slow flushing conditions) and a third one located outside, in deeper waters and subject to faster flushing. Regarding the farm size, the average historical production that took place in the period 2000–2007 was considered. The study presents the farm modelling results as a percentage change in chlorophyll-a, ammonium, oxygen and nitrate between a baseline simulation (no finfish farms) and the historical farm size simulation. Results showed that the farms' impact in Kuwait Bay is minimal, with a slight increase in the concentration of nutrients (0.4% at maximum for ammonium and nitrate), slightly raising the chlorophyll-a and oxygen concentration (less than 1%).

This study suggests that the impacts of larger farms can be mitigated by choosing a location subject to faster flushing. By understanding the interactions between finfish farms and the surrounding environment, it is possible to predict and estimate their impacts, which can be used for both mitigation and management of marine ecosystem purposes.

Author Contributions: Conceptualization, M.A.V.C.A., L.G.-G. and J.A.; Methodology, M.A.V.C.A., L.G.-G. and J.A.; Writing—Original draft, M.A.V.C.A., L.G.-G. and J.A.; Writing—Review & editing, M.A.V.C.A., L.G.-G. and J.A. All authors have read and agreed to the published version of the manuscript.

Funding: This research was funded by Cefas through the Seedcorn project DP409A.

Institutional Review Board Statement: Not applicable.

Informed Consent Statement: Not applicable.

Data Availability Statement: Not applicable.

Acknowledgments: The authors would like to thank the Kuwait Environment Public Authority (KEPA) and the Kuwait Institute for Scientific Research (KISR) for the field data. This work was carried out on the High-Performance Computing Cluster supported by the Research and Specialist Computing Support service at the University of East Anglia and the Centre for Sustainable Use of the Seas at the University of East Anglia.

Conflicts of Interest: The authors declare no conflict of interest.

References

1. Godfray, H.C.J.; Beddington, J.R.; Crute, I.R.; Haddad, L.; Lawrence, D.; Muir, J.F.; Pretty, J.; Robinson, S.; Thomas, S.M.; Toulmin, C. Food security: The challenge of feeding 9 billion people. *Science* **2010**, *327*, 812–818. [CrossRef] [PubMed]
2. Béné, C.; Barange, M.; Subasinghe, R.; Pinstrup-Andersen, P.; Merino, G.; Hemre, G.I.; Williams, M. Feeding 9 billion by 2050—Putting fish back on the menu. *Food Secur.* **2015**, *7*, 261–274. [CrossRef]
3. Thilsted, S.H.; Thorne-Lyman, A.; Webb, P.; Bogard, J.R.; Subasinghe, R.; Phillips, M.J.; Allison, E.H. Sustaining healthy diets: The role of capture fisheries and aquaculture for improving nutrition in the post-2015 era. *Food Policy* **2016**, *61*, 126–131. [CrossRef]
4. Price, C.; Black, K.D.; Hargrave, B.T.; Morris, J.A. Marine cage culture and the environment: Effects on water quality and primary production. *Aquac. Environ. Interact.* **2014**, *6*, 151–174. [CrossRef]

5. Murad, H. State of Kuwait: National Review on Marine Cage Aquaculture. *FAO Fisheries and Aquaculture Report No. 892 FIMA/R892 (En)*. 2009. Available online: http://www.fao.org/3/a-i0723e.pdf (accessed on 5 February 2018).
6. Alosairi, Y.; Alsulaiman, N. Hydro-environmental processes governing the formation of hypoxic parcels in an inverse estuarine water body: Model validation and discussion. *Mar. Pollut. Bull.* **2019**, *144*, 92–104. [CrossRef]
7. FAO. 2019. Available online: http://www.fao.org/fishery/countrysector/naso_kuwait/en (accessed on 15 December 2019).
8. Pokavanich, T.; Alosairi, Y. Summer flushing characteristics of Kuwait Bay. *J. Coast. Res.* **2014**, *30*, 1066–1073. [CrossRef]
9. Reynolds, M. Physical oceanography of the Gulf, Strait of Hormuz, and the Gulf of Oman: Results from the Mt. Mitchell Expedition. *Mar. Pollut. Bull.* **1993**, *27*, 35–59. [CrossRef]
10. Alosairi, Y.; Pokavanich, T. Residence and transport time scales associated with Shatt Al-Arab discharges under various hydrological conditions estimated using a numerical model. *Mar. Pollut. Bull.* **2017**, *118*, 85–92. [CrossRef]
11. Al-Said, T.; Al-Ghunaim, A.; Subba Rao, D.V.; Al-Yamani, F.; Al-Rifaie, K.; Al-Baz, A. Salinity-driven decadal changes in phytoplankton community in the NW Arabian Gulf of Kuwait. *Env. Monit Assess* **2017**, *189*, 268. [CrossRef]
12. Alajmi, H.M. Effect of Physical, Chemical and Biological Treatment on the Removal of Five Pharmaceuticals from Domestic Wastewater in Laboratory-Scale Reactors and a Full-Scale Plant. Ph.D. Thesis, University of Newcastle, Newcastle, Australia, 2014.
13. Pokavanich, T.; Polikarpov, I.; Lennox, A.; Al-Hulail, F.; Al-Said, T.; Al-Enezi, E.; Al-Yamani, F.; Stokozov, N.; Shuhaibar, B. Comprehensive investigation of summer hydrodynamic and water quality characteristics of desertic shallow water body: Kuwait Bay. In Proceedings of the 7th International Conference on Coastal Dynamics, Arcachon, France, 23–26 June 2013; pp. 1253–1264.
14. Alosairi, Y.; Pokavanich, T.; Alsulaiman, N. Three-dimensional hydrodynamic modelling study of reverse estuarine circulation: Kuwait Bay. *Mar. Pollut. Bull.* **2018**, *127*, 82–96. [CrossRef]
15. Al-Yamani, F.; Subba Rao, D.; Mharzi, A.; Ismail, W.; Al-Rifaie, K. Primary production off Kuwait, an arid zone environment, Arabian Gulf. *Int. J. Ocean. Oceanogr.* **2006**, *1*, 67–85.
16. Al-Yamani, F. Importance of the freshwater influx from the Shatt-AlArab River on the Gulf marine environment. In *Protecting the Gulf's Marine Ecosystems from Pollution*; Abuzinada, A.H., Barth, H.-J., Krupp, F., Böer, B., Al Abdessalaam, T.Z., Eds.; Birkhäuser Verlag: Basel, Switzerland, 2008.
17. Subba Rao, D.; Al-Yamani, F. Phytoplankton ecology in the waters between Shatt-Al-Arab and Straits of Hormuz-the Arabian Gulf. *Plankton Biol. Ecol.* **1998**, *45*, 101–116.
18. Devlin, M.J.; Breckels, M.; Graves, C.A.; Barry, J.; Capuzzo, E.; Huerta, F.P.; Al Ajmi, F.; Al-Hussain, M.M.; LeQuesne, W.J.F.; Lyons, B.P. Seasonal and Temporal Drivers Influencing Phytoplankton Community in Kuwait Marine Waters: Documenting a Changing Landscape in the Gulf. *Front. Mar. Sci.* **2019**, *6*, 141. [CrossRef]
19. Devlin, M.; Massoud, M.; Hamid, S.; Al-Zaidan, A.; Al-Sarawi, H.; Al-Enezi, M.; Al-Ghofran, L.; Smith, A.; Barry, J.; Stentiford, G.; et al. Changes in the water quality conditions of Kuwait's marine waters: Long term impacts of nutrient enrichment. *Mar. Pollut. Bull.* **2015**, *100*, 607–620. [CrossRef] [PubMed]
20. Deltares. *Delft3D-FLOW. Hydro-Morphodynamics User Manual*; Version 3.15; Deltares: Delft, The Netherlands, 2014.
21. Bacon, J.; Phillips, R. Rehabilitaion of Impacted Marine Areas in Kuwait. In *Cefas Interim Report: Numerical Modelling of Kuwait Bay 2014*; Cefas: Suffolk, UK, 2014; not publicly available.
22. Todd Navigation. Admiralty Chart—2884 Mina' Az Zawr to Al Basrah & Bushehr,2014. AC2884 UKHO. Available online: https://www.toddchart.com/Products/Admiralty-Chart-2884-Mina-Az-Zawr-To-Al-Basrah-and-Bushehr/AC2884 (accessed on 20 July 2016).
23. Zuo, H.; Balmaseda, M.A.; Mogensen, K. The new eddy-permitting ORAP5 ocean reanalysis: Description, evaluation and uncertainties in climate signals. *Clim. Dyn.* **2017**, *49*, 791–811. [CrossRef]
24. Dai, A.; Trenberth, K.E. Estimates of freshwater discharge from continents: Latitudinal and seasonal variations. *J. Hydrometeorol.* **2002**, *3*, 660–687. [CrossRef]
25. Kampf, J.; Sadrinasab, M. The circulation of the Persian Gulf: A numerical study. *Ocean Sci.* **2006**, *2*, 27–41. [CrossRef]
26. Alosairi, Y.; Pokavanich, T. Seasonal circulation assessments of the Northern Arabian/Persian Gulf. *Mar. Pollut. Bull.* **2017**, *116*, 270–290. [CrossRef]
27. Dee, D.P.; Uppala, S.M.; Simmons, A.J.; Berrisford, P.; Poli, P.; Kobayashi, S.; Andrae, U.; Balmaseda, M.A.; Balsamo, G.; Bauer, P.; et al. The ERA-Interim reanalysis: Configuration and performance of the data assimilation system. *Q. J. R. Meteorol. Soc.* **2011**, *137*, 553–597. [CrossRef]
28. Elhakeem, A.; Elshorbagy, W.; Bleninger, T. Long-term hydrodynamic modeling of the Arabian Gulf. *Mar. Pollut. Bull.* **2015**, *94*, 19–36. [CrossRef]
29. Van Rijn, L.C.; Walstra, D.J.R.; Grasmeijer, B.; Sutherland, J.; Pan, S.; Sierra, J.P. Simulation of nearshore hydrodynamics and morphodynamics on the time scale of storms and seasons using process-based profile models. In *The Behaviour of a Straight Sandy Coast on the Time Scale of Storms and Seasons: Process Knowledge and Guidelines for Coastal Management*; EC MAST Project, MAS3-CT97-0086 COAST3D–EGMOND; Van Rijn, L.C., Ruessink, B.G., Mulder, J.P.M., Eds.; Vliz.be: Ostend, Belgium, 2002.
30. Deltares. D-Water Quality. In *Versatile Water Quality Modelling in Delta Shell User Manual*; Version 1.1; Deltares: Delft, The Netherlands, 2019.
31. Pokavanich, T.; Alosairi, Y.; Reimer De Graaff Morelissen, R.; Verbruggen, W.; Al-Rifaie, K.; Altaf, T.; Al-Said, T. Three-dimensional Arabian Gulf hydro-environmental modeling using Delft3D. In Proceedings of the 36th IAHR World Congress 2015, The Hague, The Netherlands, 28 June—3 July 2015.

32. Ministry of Environment-Iraq. The Marshes-Shatt al-Arab-Gulf System; Status Report; Volume 1. *Marine Science Centre 2011–University of Basra.* Available online: https://wedocs.unep.org/handle/20.500.11822/8849 (accessed on 6 September 2017).
33. Hassam, W. The nitrogen and phosphate forms in water of Shatt Al-Arab River in Basra/Iraq. *Marsh Bull.* **2013**, *8*, 182–192.
34. Al-Muzaini, S. Management of land-based sources of marine pollution. *Aquat. Ecosyst. Health Manag.* **2013**, *16*, 347–356. [CrossRef]
35. Aleisa, E.; Alshayji, K. Analysis on Reclamation and Reuse of Wastewater in Kuwait. *J. Eng. Res.* **2019**, *7*, 1–13.
36. FAO. Irrigation in the Middle East Region in Figures: AQUASTAT Survey, 2008 Water Report 34. Available online: http://www.fao.org/docrep/012/i0936e/i0936e00.htm (accessed on 15 October 2017).
37. Dubber, D.; Gray, N.F. Replacement of chemical oxygen demand (COD) with total organic carbon (TOC) for monitoring wastewater treatment performance to minimize disposal of toxic analytical waste. *J. Environ. Sci. Health Part A* **2010**, *45*, 1595–1600. [CrossRef]
38. Hua, X.; Song, X.; Yuan, M.; Donga, D. The Factors Affecting Relationship between COD and TOC of Typical Papermaking Wastewater. In *Advances in Computer Science, Intelligent System and Environment. Advances in Intelligent and Soft Computing*; Jin, D., Lin, S., Eds.; Springer: Berlin/Heidelberg, Germany, 2011; Volume 105.
39. Duan, H.; Feng, L.; Ma, R.; Zhang, Y.; Loiselle, S.A. Variability of particulate organic carbon in inland waters observed from MODIS Aqua imagery. *Environ. Res. Lett.* **2014**, *9*, 084011. [CrossRef]
40. Islam, M.S. Nitrogen and phosphorus budget in coastal and marine cage aquaculture and impacts of effluent loading on ecosystem: Review and analysis towards model development. *Mar. Pollut. Bull.* **2005**, *50*, 48–61. [CrossRef]
41. Reid, G.K.; Liutkus, M.; Robinson, S.M.C.; Chopin, T.R.; Blair, T.; Lander, T.; Mullen, J.; Page, F.; Moccia, R.D. A review of the biophysical properties of salmonid faeces: Implications for aquaculture waste dispersal models and integrated multi-trophic aquaculture. *Aquac. Res.* **2009**, *40*, 257–273. [CrossRef]
42. Wang, X.; Olsen, L.M.; Reitan, K.I.; Olsen, Y. Discharge of nutrient wastes from salmon farms: Environmental effects, and potential for integrated multi-trophic aquaculture. *Aquac. Environ. Interact.* **2012**, *2*, 267–283. [CrossRef]
43. Bouwman, A.F.; Beusen, A.H.W.; Overbeek, C.C.; Bureau, D.P.; Pawlowski, M.; Glibert, P.M. Hindcasts and future projections of global inland and coastal nitrogen and phosphorus loads due to finfish aquaculture. *Rev. Fish. Sci.* **2013**, *21*, 112–156. [CrossRef]
44. Wang, X.; Andresen, K.; Handå, A.; Jensen, B.; Reitan, K.I.; Olsen, Y. Chemical composition and release rate of waste discharge from an Atlantic salmon farm with an evaluation of IMTA feasibility. *Aquac. Environ. Interact.* **2013**, *4*, 147–162. [CrossRef]
45. Pokavanich, T.; Alosairi, Y. Measurement of seasonal variability of hydro-environmental characteristics of Kuwait Bay. *Arab J. Geosci.* **2016**, *9*, 671. [CrossRef]